Available online at www.sciencedirect.com
ScienceDirect
Polymer 48 (2007) 870–876
polymer
www.elsevier.com/locate/polymer

# Conformation transition and crystalline phase variation of long chain branched isotactic polypropylenes (LCB-iPP)

Zhiqiang Su [a,b], Hongying Wang [a], Jinyong Dong [a], Xiuqin Zhang [a], Xia Dong [a], Ying Zhao [a], Jian Yu [b,**], Charles C. Han [a], Duanfu Xu [a], Dujin Wang [a,*]

[a] *Beijing National Laboratory for Molecular Sciences, CAS Key Laboratory of Engineering Plastics, Joint Laboratory of Polymer Science and Materials, Institute of Chemistry, Chinese Academy of Sciences, Beijing 100080, China*

[b] *Institute of Polymer Science and Engineering, Department of Chemical Engineering, School of Materials Science and Engineering, Tsinghua University, Beijing 100084, China*

Received 11 November 2006; received in revised form 11 December 2006; accepted 12 December 2006
Available online 2 January 2007

**Abstract**

The changes of conformation and crystalline structure of long chain branched isotactic polypropylene (LCB-iPP) under different crystallization temperatures and the effects of their special molecular architecture on the crystallization behavior were investigated by a combination of Fourier transform infrared spectroscopy (FT-IR), wide-angle X-ray diffraction (WAXD) and differential scanning calorimetry (DSC). In these polymers, long chain branching was introduced via in situ polymerization of polypropylene and an asymmetric diene monomer using the metallocene catalyst technology. Through the characterization of the specific IR band variation, it was proved that the conformational orders of helical sequences of LCB-iPP show great changes in different crystallization temperature ranges. In lower crystallization temperature range (100–130 °C), the intensities of all regular helical conformation bands of LCB-iPP increase with the increasing crystallization temperature and the regular helical conformation bands with more monomer units increase faster than that with less monomer units. In higher crystallization temperature range (130–150 °C), the intensities of all regular helical conformation bands of LCB-iPP decrease with the increasing crystallization temperature and the regular helical conformation bands with more monomer units decrease faster than that with less monomer units. The results of WAXD and DSC showed that LCB-iPP crystallizes from the melt as a mixture of α and γ forms. The content of the γ form increases with the increasing crystallization temperature, reaches a maximum value at 130 °C, and then decreases with a further increase of the temperature. At the same time, the crystallization of γ form is favored by the presence of the LCB structure of iPP. Moreover, the transitional temperatures of different helical conformations and crystallization structures of LCB-iPP show obvious correlations.
© 2006 Elsevier Ltd. All rights reserved.

*Keywords:* Long chain branched isotactic polypropylene; Conformation transition; Crystallization behavior

## 1. Introduction

Isotactic polypropylene is a useful thermoplastic with a wide range of applications. Nevertheless, the iPP, no matter prepared by Ziegler–Natta or metallocene catalysts, has a predominantly linear molecular structure and shows a variety of melt-processing shortcomings. The low melt strength causes local instability in thermoforming, blow molding, extrusion coating and foaming [1–3]. As a result, iPP has been limited in some end-use fabrications. Through the utilization of metallocene catalyst technology, many structure features, including long chain branching (LCB), can be introduced into polymer chains during polymerization. The LCB structure can improve the processing ability of iPP under melt condition, including strain hardening, shear thinning, high melt strength and so on, thus broadening the end uses and processing methods of polypropylene [4–8].

* Corresponding author. Tel.: +86 10 82616255; fax: +86 10 82612857.
** Corresponding author.
*E-mail addresses:* yujian03@mail.tsinghua.edu.cn (J. Yu), djwang@iccas.ac.cn (D. Wang).

0032-3861/$ - see front matter © 2006 Elsevier Ltd. All rights reserved.
doi:10.1016/j.polymer.2006.12.013

Because of its special chain structure, LCB-iPP is believed to show different helical conformation and crystallization structure in the process of crystallization. The different helical conformation and complicated crystallization structure will greatly influence the processing ability of LCB-iPP. However, up to now, there are few articles investigating the conformation and crystallization structure of LCB-iPP under different crystallization conditions.

FT-IR spectroscopy is sensitive to the constitution and the folding manner of molecular chains, and can provide much meaningful structural information. It is an effective method for characterizing the changes of helical conformation of iPP [9–11]. For iPP, most absorption bands in the mid-infrared region originate from the intramolecular coupling of the oscillations of the various atomic groups within a single chain [12]. On this basis, during the past decade, the relationship between specific regularity bands of FT-IR spectrum and the different helical conformation length "*n*" of iPP has been well established [13–19]. The minimum *n* values for the appearance of bands at 973, 998, 840 and 1220 $cm^{-1}$ are 2–4, 5–10, 12–14 and 14 or more monomers units in helical sequences, respectively. Apparently, larger the *n* value, higher the ordered degree of the corresponding regularity is. Therefore, the information of conformational change of LCB-iPP during the crystallization process can be obtained by calculating the absorbance ratios of different regularity bands in FT-IR spectra.

It has been reported that for iPP samples prepared with metallocene catalysts, a mixture of the α and γ forms is obtained by isothermal crystallization from the melt, and the content of γ form increases with increasing the content of defects [20–22]. The data published so far [20–26] indicated that when the fully isotactic sequences are very short, iPP crystallizes in the γ form, whereas very long regular isotactic sequences generally crystallizes only in the α form. Weng analyzed the LCB structures in the LCB-iPP in detail with $^{13}C$ NMR, and pointed out that the incorporation of LCB structures in the LCB-iPP will bring stereo mistakes (mr and rr) in isotactic backbone structures [27]. As a result, the LCB structure will influence the final phase structure of LCB-iPP. At the same time, the crystallization temperatures will change the helical conformation regularity and ultimately affect the crystallization structure of LCB-iPP. Up to date, however, the crystallization behavior of LCB-iPP samples has not been well understood.

Therefore, the main aim of the present work is to understand the structure–property correlations of LCB-iPP in-depth through characterizing the changes of conformation, polymorphism and phase transformation in the process of crystallization. The variation mechanism of conformation and crystalline structure of LCB-iPP and the relationships among them have also been discussed.

## 2. Experimental section

### 2.1. Materials and sample preparation

The LCB-iPP samples were synthesized following a new polymerization process [28]. Samples with different long branched chains were in situ prepared by one-pot polymerization process, which employs a novel branching reagent, i.e., *p*-(3-butenyl) styrene, as illustrated in Scheme 1. This asymmetric diene serves as both co-monomer and transfer agent during metallocene-mediated propylene polymerization, using isospecific *rac*-$SiMe_2$[2-Me-4-(1-NaPh)Ind]$_2ZrCl_2$/MAO catalyst in the presence of a small amount of hydrogen. Desired molecular weight ($M_w$), branching degree and melt flow rate (MFR) of the samples were achieved by controlling the reaction conditions. The basic physical parameters of LCB-iPP were listed in Table 1.

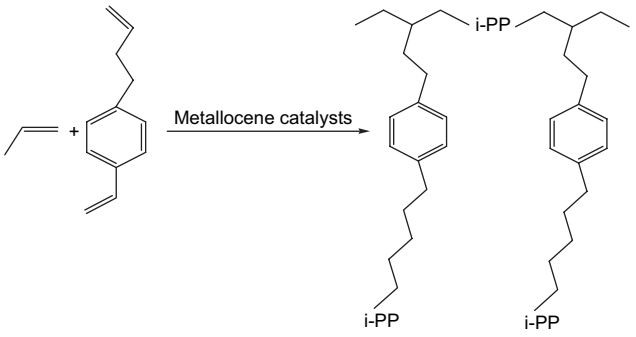


Scheme 1. Preparation of long chain branched isotactic polypropylene.

In order to investigate the influence of thermal history on the conformation and the crystalline structure of LCB-iPP, the samples were isothermally crystallized from the melt at different temperatures. For sample preparation, it is not sufficient to consider only the crystallization condition, but sample size and shape should also be taken into consideration. For example, the actual thermal history of samples with different thickness varied greatly. In this work, all the samples were first sandwiched between two aluminum flakes and melt-pressed to form a film with a thickness of ca. 100 μm. The compression-molded specimens were then melted at 220 °C and kept for 10 min to erase any thermal history, followed by rapidly cooled to a specific crystallization temperature ($T_c$) and kept at this temperature for 48 h to allow isothermal crystallization. The final samples were then rapidly cooled to room temperature and analyzed by WAXD, DSC and FT-IR methods. Several isothermal crystallization temperatures were adopted, $T_c = 100$, 110, 120, 130, 140, and 150 °C.

### 2.2. Characterization

*FT-IR*: IR spectra of all samples were measured at 26 °C using a Nicolet Magna 750 FT-IR spectrometer equipped with a DTGS detector. The spectra were collected at a resolution of

Table 1
Basic parameters of LCB-iPP samples

| Samples | Diene content (mol) | Hydrogen content (mmol) | Branching degree (%) | $M_n$ | $M_w$ | $T_m$ (°C) |
|---|---|---|---|---|---|---|
| R1 | 4.81E − 03 | 11.90 | 0.46 | 3.03E4 | 2.33E5 | 148.1 |
| R2 | 2.41E − 03 | 2.40 | 0.25 | 2.53E4 | 1.63E5 | 144.1 |

4 $cm^{-1}$ with 16 scans. The measured wavenumber range was 400–4000 $cm^{-1}$. All the original spectra were baseline corrected using OMNIC 5.1 software before curve fitting.

*WAXD*: All WAXD experiments were performed at room temperature using a PaNalytical (Holand) X′ pert Pro MRD diffractometer (Cu Kα, $\lambda = 0.154$ nm, 40 kV, 40 mA, reflection mode). The experiments were performed with a $2\theta$ range of 5–30°, a scanning rate of 2°/min, and a scanning step of 0.02°.

*DSC*: The calorimetric measurements of all samples were carried out with a Mettler DSC 822e differential scanning calorimeter at a scan rate of 10 °C/min under a flowing $N_2$ atmosphere, and the sample weight was ca. 10 mg. Indium was used as the standard sample.

## 3. Results and discussion

### 3.1. Effect of crystallization temperatures on the conformation structure of LCB-iPP

As described in Section 1, the regularity IR bands of the polymers originate from the intramolecular coupling of the oscillations of various atomic groups [12]. These bands are related to different helical lengths of isotactic sequences [13–19]. Therefore, the conformational ordering of different LCB-iPP samples can be determined by the absorbance ratio of the various regularity bands.

Figs. 1 and 2 show the FT-IR spectra of two kinds of LCB-iPP samples (R1 and R2) with different branching degrees under different crystallization temperatures. It was observed that the intensities of different regularity bands (973, 998, 841, 1220 $cm^{-1}$) change slightly with increasing the crystallization temperature. Since each IR band has its own intensity coefficient, the intensities of these regular helical conformation bands should be normalized. Because the IR band at 1460 $cm^{-1}$ corresponding to the asymmetric deformation vibration of the methyl group is almost not influenced by the variation of external environment, it can serve as an internal standard [10,11,29]. The normalized intensity variation of the different regularity bands of R1 and R2 samples, calculated from the IR spectra

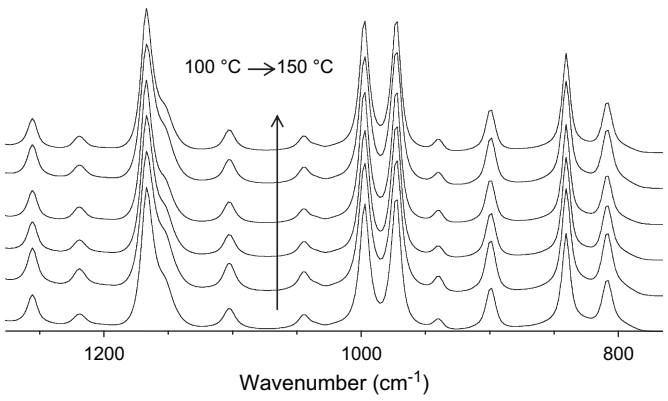


Fig. 1. FT-IR spectra of sample R1 crystallized from different temperatures.

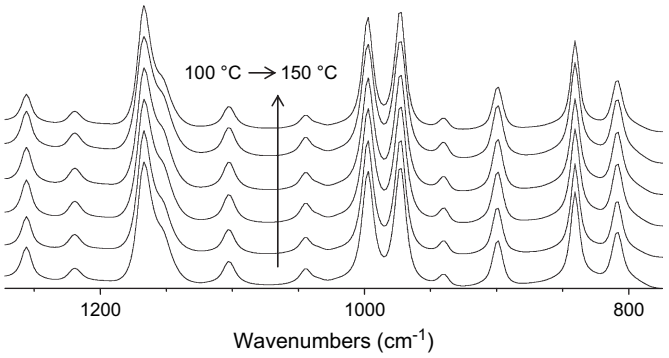


Fig. 2. FT-IR spectra of sample R2 crystallized from different temperatures.

of Figs. 1 and 2, is shown in Figs. 3 and 4, respectively, as a function of crystallization temperature.

Figs. 3 and 4 show that the trends for the intensity variation of different regularity bands with crystallization temperature are similar, i.e., the intensity of all these bands first increases and then decreases above a certain crystallization temperature. As $T_c$ increases from 100 to 120 °C, the crystalline perfection of LCB-iPP increases gradually, so the intensity of all the helical conformation bands of LCB-iPP increases, especially, the intensity of the helical conformation bands with more monomer units increases more rapidly. As temperature increases from 120 to 130 °C, the intensity of the helical band at 1220 $cm^{-1}$ with more than 14 monomer units still increases with increasing crystallization temperature and reaches a maximum at 130 °C, while the intensities of all the other regular helical bands (840, 998, 973 $cm^{-1}$) with less monomer units continue to decrease after 120 °C. It is interesting that the intensity of 840 $cm^{-1}$ band with 12–14 monomer units decreases slower than that of 998 and 973 $cm^{-1}$ bands with less than 10 monomer units, implying that the shorter helical conformation sequences might gradually translate into the longer helical conformation sequence in LCB-iPP samples with increasing crystallization temperature. With further

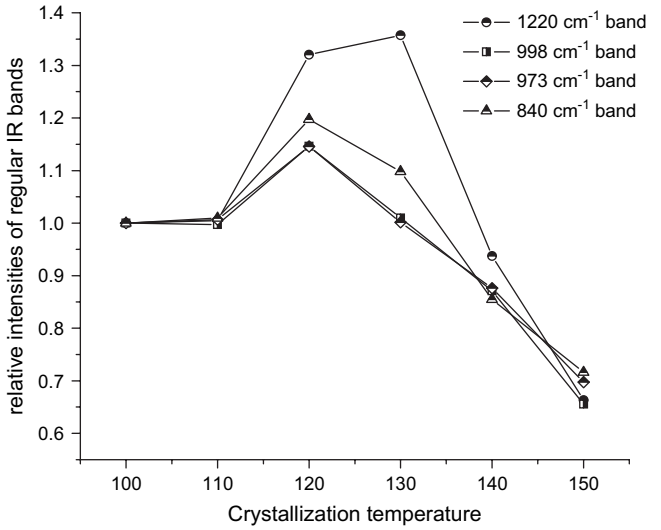


Fig. 3. Intensity variation of different regularity bands of R1 sample, calculated from the IR spectra of Fig. 1, as a function of the crystallization temperature. The intensity of all the bands at 100 °C was taken as the reference.

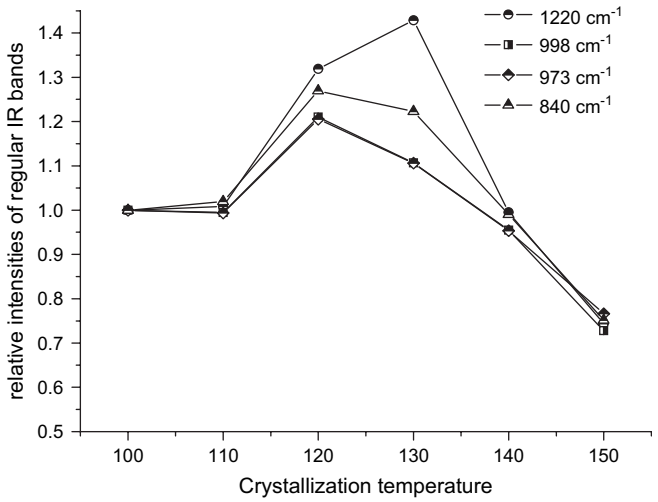


Fig. 4. Intensity variation of different regularity bands of R2 sample, calculated from the IR spectra of Fig. 2, as a function of the crystallization temperature. The intensity of all the bands at 100 °C was taken as the reference.

increasing of the crystallization temperature from 130 to 150 °C, the intensities of all the helical bands of LCB-iPP decrease with $T_c$. Among them, the intensity of 1220 $cm^{-1}$ band decreases very quickly, the 840 $cm^{-1}$ is the second one, and the intensity of 998 and 973 $cm^{-1}$ bands decreases very slowly. The above intensity variation indicates that the longer helical conformation sequences in LCB-iPP samples are destroyed at higher $T_c$, which is close to the melting temperature. As a result, the conformational order and the crystallization ability of LCB-iPP decrease. Comparing Figs. 3 and 4, it can be observed that the conformation changing tendency of R1 with $T_c$ is similar to that of R2.

Figs. 5 and 6 show the intensity ratios of different regularity bands of samples R1 and R2, respectively, as a function of $T_c$.

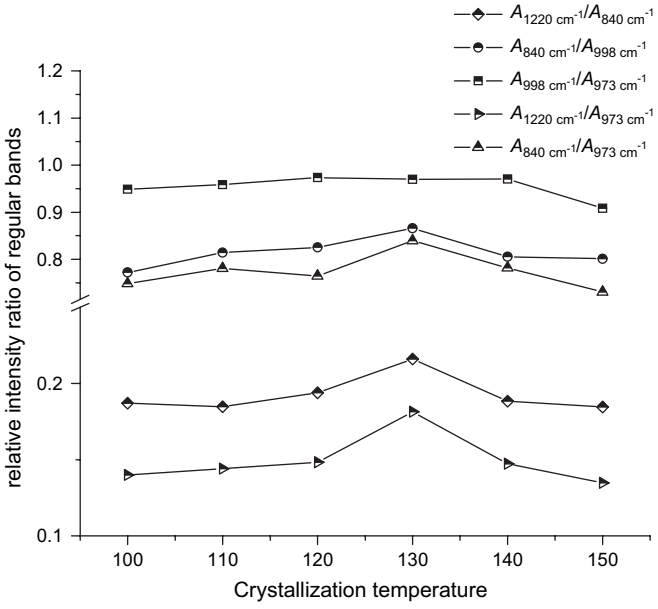


Fig. 5. Relative intensity ratios of different regularity bands of sample R1 versus the crystallization temperature.

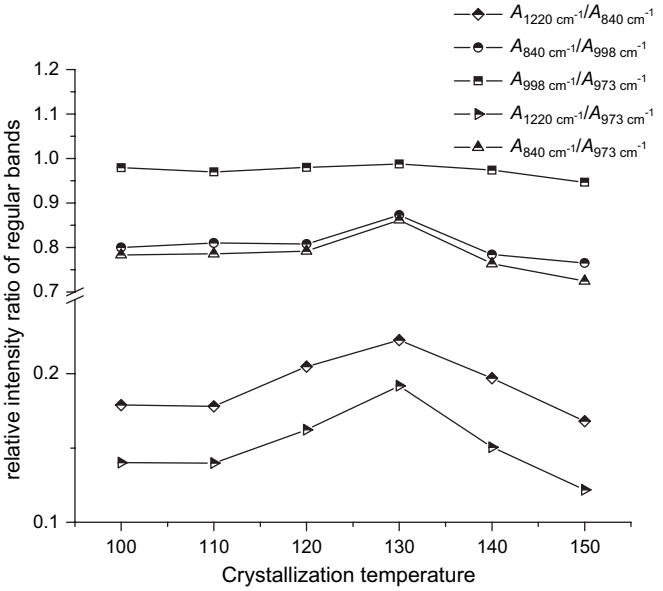


Fig. 6. Relative intensity ratios of different regularity bands of sample R2 versus the crystallization temperature.

It can be observed that the relative intensity ratios of $A_{998\ cm^{-1}}/A_{973\ cm^{-1}}$, $A_{840\ cm^{-1}}/A_{973\ cm^{-1}}$ and $A_{1220\ cm^{-1}}/A_{973\ cm^{-1}}$ all increase with $T_c$, reaches a maximum value at 130 °C, and then decreases as crystallization temperature further increases. Furthermore, with the increase of $T_c$, the intensity ratios of $A_{1220\ cm^{-1}}/A_{840\ cm^{-1}}$ and $A_{840\ cm^{-1}}/A_{998\ cm^{-1}}$ show the same changing tendency. The above results indicated that the conformational ordering of the helical sequences of LCB-iPP changes a lot in the range of the crystallization temperature. At lower $T_c$ (100–130 °C), the intensities of all the regular bands of LCB-iPP increase with temperature, among which the bands with more monomer units increase more quickly. At higher $T_c$ (130–150 °C), the intensities of all regular bands of LCB-iPP decrease with increasing crystallization temperature, and the bands with more monomer units decrease more quickly.

### 3.2. Variation of crystallization structure of LCB-iPP under different $T_c$s

As mentioned above, the helical conformation order of LCB-iPP will change greatly under different $T_c$s. The changing of helical conformation order within a single helical chain may influence the regular spatial arrangements of other helical chains of LCB-iPP, thus causing the variation of crystalline structure of LCB-iPP. Consequently, the crystalline structure will greatly influence the processibility of LCB-iPP. In this section, the transformation of crystallization structures of LCB-iPP with $T_c$ was investigated by WAXD and DSC.

The WAXD profiles of samples R1 and R2 isothermally crystallized from the melt at different temperatures are shown in Figs. 7 and 8, respectively. For LCB-iPP samples, the α and γ forms present very similar WAXD profiles, the main difference being the position of the third strong diffraction peak,

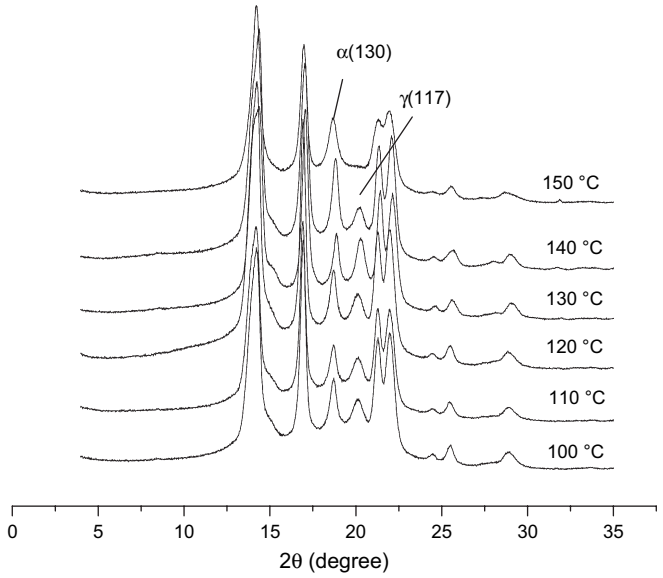


Fig. 7. WAXD profiles of LCB-iPP sample R1 isothermally crystallized from melt at the indicated temperatures.

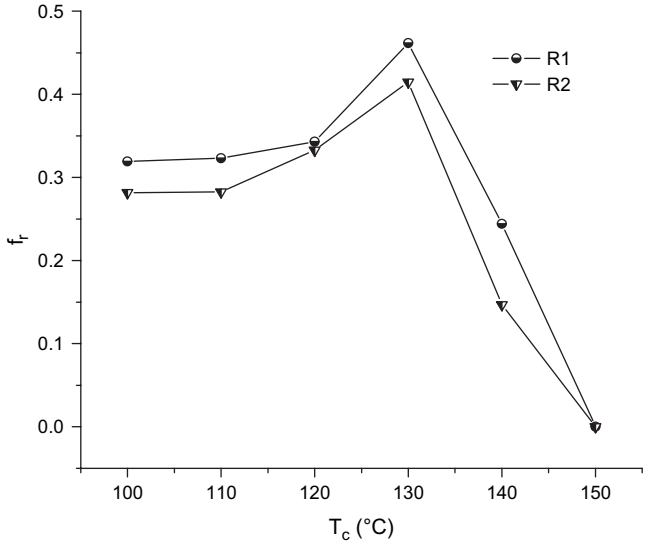


Fig. 9. Content of γ form of LCB-iPP samples, evaluated from the WAXD profiles, as a function of the crystallization temperature.

which occurs at $2\theta = 18.6°$ ($(130)_\alpha$ reflection) in the α form [30], and at $2\theta = 20.1°$ ($(117)_\gamma$ reflection) in the γ form [31,32]. The presence of the diffraction peaks at $2\theta = 18.6°$ and 20.1° in the WAXD profiles of R1 and R2 samples indicates that these samples crystallize in a mixture of two crystal forms, both α and γ forms develop by crystallization from the melt. The relative content of crystals in the γ form presented in our samples was measured from the WAXD profiles, as suggested by Turner-Jones et al. [33], by measuring the ratio between the intensities of the $(117)_\gamma$ reflection at $2\theta = 20.1°$, typical of the γ form, and the $(130)_\alpha$ reflection at $2\theta = 18.6°$, typical of the α form

$$f_\gamma = I(117)_\gamma / \left[ I(130)_\alpha + I(117)_\gamma \right]$$

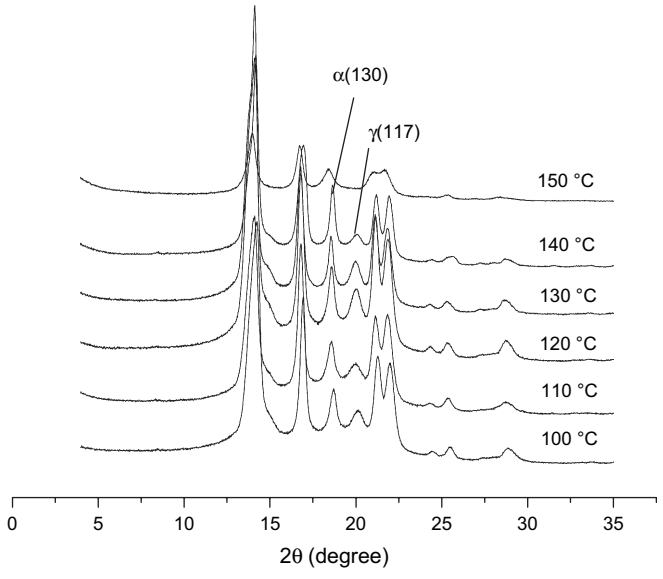


Fig. 8. WAXD profiles of LCB-iPP sample R2 isothermally crystallized from melt at the indicated temperatures.

where $I(130)_\alpha$ and $I(117)_\gamma$ present the intensities of $(130)_\alpha$ and $(117)_\gamma$ reflections, respectively, in the WAXD profiles obtained by curve-fitting techniques.

The relative content of the γ form with respect to the α form, $f_r$, is reported in Fig. 9 as a function of $T_c$. The calculated results showed that the value of $f_r$ increases with increasing crystallization temperature, reaching a maximum at 130 °C, and then decreases with the further increase of $T_c$. When $T_c$ rose up to 150 °C, the γ form disappears completely. The occurrence of maxima in the curves of $f_r$ may be explained by the competing effect of kinetics and thermodynamics. For our synthesized LCB-iPP samples containing an appreciable amount of stereodefects, the formation of the γ form is thermodynamically favored, since the structural defects are highly tolerated in the γ form, less in the crystals of the α form [20,34]. As a consequence, a high amount of the γ form develops under slow crystallization rates at higher temperatures. Under lower $T_c$, the fast crystallization of the α form is instead kinetically favored, giving a low amount of γ form. With $T_c$ increasing, the amount of γ form increases, but at very high crystallization temperatures (higher than 130 °C) the crystallization of the γ form is too slow because of its lower melting temperature [20], and the α form becomes again kinetically favored, so that the amount of γ form decreases.

It is also apparent in Fig. 9 that the content of the γ form present in sample R1 is always higher than that of sample R2. This can be explained by the structural difference of these two samples. The increase in the content of LCB structures in LCB-iPP samples will bring stereo mistakes (mr and rr) in isotactic backbone structures [27] while the formation of the γ form is favored by the presence of stereodefects and regiodefects [20–22]. Due to the relatively high LCB structure in sample R1, its γ form content from different crystallization temperatures is always bigger than that of sample R2.

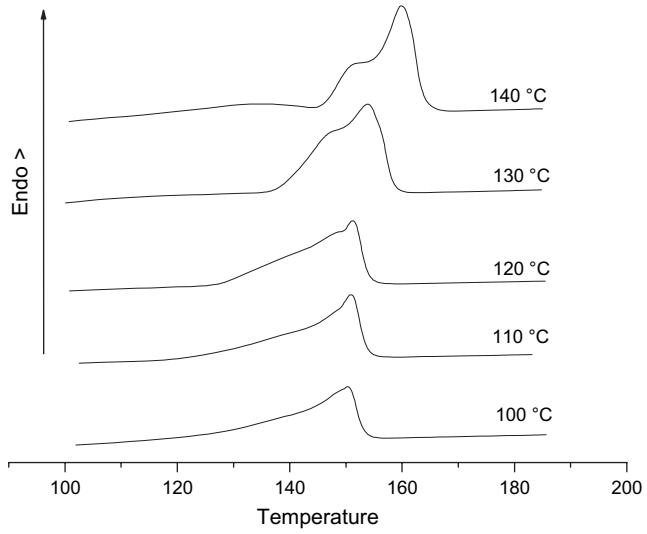


Fig. 10. DSC heating thermograms of sample R1, isothermally crystallized at different $T_c$s from the melt at the rate of 10 °C/min.

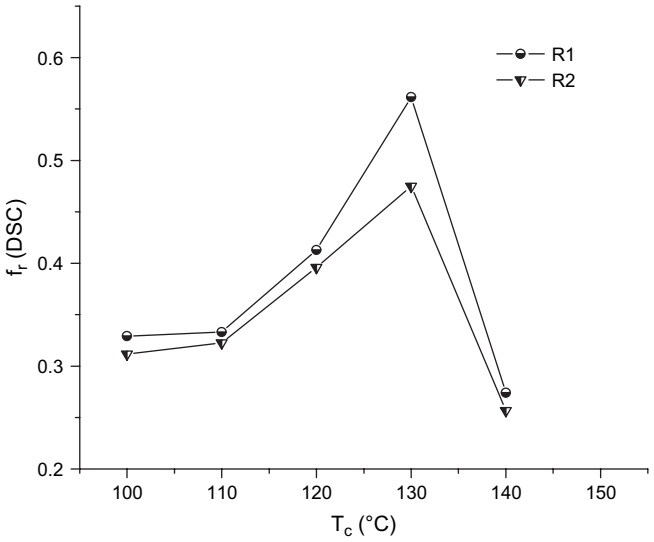


Fig. 12. Relative content of γ form of LCB-iPP, evaluated from the DSC thermograms of Figs. 10 and 11, as a function of $T_c$.

Figs. 10 and 11 show the DSC heating thermograms of samples R1 and R2, respectively, recorded at the heating rate of 10 °C/min after isothermal crystallization at different $T_c$s. All the samples show broad melting endotherms characteristic of doublet peaks. The peak at lower temperature presents as a shoulder of the peak at higher temperature. Both the melting peaks shift to higher temperature region with increasing $T_c$. The integral area of the peak at low temperature continues to increase up to $T_c = 130$ °C, which above this point, starts to decrease with further increasing of $T_c$. The melting behavior of metallocene iPP samples crystallized from the melt has been extensively studied by Alamo et al. [20]. It has been proved that the multiple peaks present in the DSC scans are due to melting of the two polymorphic forms of iPP. The γ form melts, generally, at lower temperature, and the α form at higher temperature.

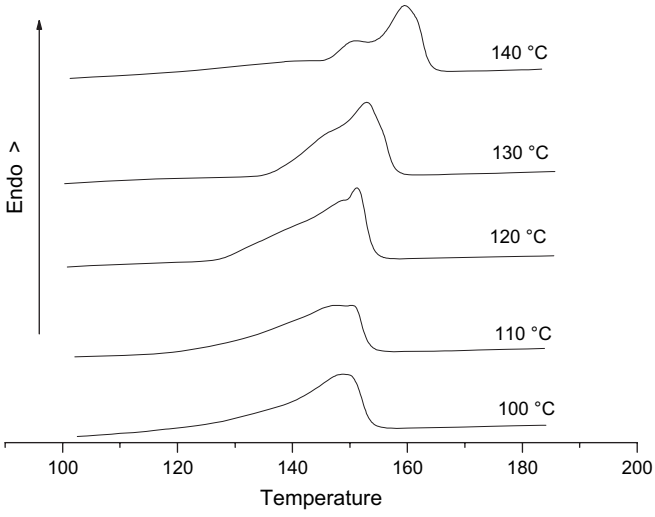


Fig. 11. DSC heating thermograms of sample R2, isothermally crystallized at different $T_c$s from the melt at the rate of 10 °C/min.

It can also be observed from Figs. 10 and 11 that the γ form melts in a rather broad range of temperature (more than 10 °C), whereas the α form melts in a range of only 3 °C. This is probably due to the fact that the crystals of γ form in LCB-iPP include a large amount of defects [34]. It is a metastable crystal form and melts at lower temperatures and in a broader range of temperature. While the crystals of α form are, instead, probably more perfect and melt at higher temperatures and in a narrower range of temperature.

Because the two melting peaks in the DSC curves of the samples LCB-iPP are attributed to the melting of the α and γ forms, it is possible to evaluate the content of γ form in these samples from the relative area of the peaks in the DSC curves: $f_{\gamma(\mathrm{DSC})} = \Delta H_\gamma / \Delta H_t$, where $\Delta H_\gamma$ is the area of the peak at low temperature and $\Delta H_t$ is the total enthalpy of melting. The values of the content of γ form so evaluated are reported in Fig. 12 as a function of $T_c$. The same behavior as that of the curves in Fig. 9 is apparent. The value of $f_{\gamma(\mathrm{DSC})}$ increases with increasing $T_c$, reaches a maximum at 130 °C, and then decreases with further increase of $T_c$. The content of the γ form present in sample R1 is always higher than that of sample R2 for the reason of higher LCB content.

Based on the above observations and discussion, it can be found that both conformation and crystallization structure of LCB-iPP samples show the same changing tendency with crystallization temperature. The transitional temperatures of different helical conformations and crystallization structures of LCB-iPP show obvious relativity.

## 4. Conclusions

We investigated the changes of conformations and crystalline structures of a new class of LCB-iPP polymers under different crystallization temperatures and the effects of their special molecular architecture on the crystallization behavior,

in which the LCB was introduced via in situ polymerization of propylene and a miniscule amount of an asymmetric diene monomer using metallocene catalyst technology. The following conclusions can be drawn.

1. Through the characterization of the variation of specific IR bands, it has been proved that the crystallization temperature has great effect on the conformational orders of LCB-iPP, and the intensities of different helical conformation of LCB-iPP show great changes in different crystallization temperature ranges. At lower $T_c$ values (100–130 °C), the intensities of all regular helical conformation bands of LCB-iPP increase with $T_c$ and reach a maximum at 130 °C. At the same time, the shorter helical conformation sequences in LCB-iPP samples gradually translate into a longer helical conformation sequence. At higher $T_c$ (130–150 °C), the $T_c$ of LCB-iPP is close to its melting temperature ($T_m$) and the helical conformation order of LCB-iPP decreases with $T_c$. The regular helical conformation bands with more monomer units decrease faster than those with less monomer units.

2. Through the investigation of the polymorphism of LCB-iPP under different crystallization temperatures by WAXD and DSC, it has been found that both $\alpha$ and $\gamma$ forms develop in LCB-iPP by crystallizing from the melt, among which the $\gamma$ form is a metastable crystal with a large amount of structural defects. The $\gamma$ form melts at a lower temperature and in a broader temperature range, while the crystals of $\alpha$ form are, instead, probably more perfect and melt at higher temperatures and in a narrower temperature range. The content of the $\gamma$ form increases with $T_c$, reaching a maximum value at 130 °C, and then decreases with further increasing of $T_c$. The crystallization of $\gamma$ form is favored by the presence of the LCB in iPP.

3. The transitional temperatures of different helical conformations and crystallization structures of LCB-iPP are in good consistency.

## Acknowledgment

The financial support from National Natural Science Foundation of China (NSFC, Grant no. 50390090) and Directional Project from CAS (KJCX2-SW-H07) is greatly acknowledged.

## References

[1] Throne JL. Thermoforming. Munich: Hanser Publishers; 1987.
[2] Rosato DV. In: Rosato DV, editor. Blow molding handbook. Munich: Hanser Publishers; 1989. p. 529.
[3] McDonald JN. Thermoforming. In: Encyclopedia of polymer science and engineering, vol. 16. New York: John Wiley & Sons; 1989. p. 807.
[4] Lu B, Chung TC. Macromolecules 1999;32:8678.
[5] Roovers J. Macromolecules 1991;24:5895.
[6] Billmeyer Jr FW. Textbook of polymer science. New York: John Wiley & Sons; 1984. p. 361.
[7] Small PA. Adv Polym Sci 1975;18:1.
[8] Kokko E, Malmberg A, Lehmus P, Lofgren B, Seppala JV. J Polym Sci Part A Polym Chem 2000;38:376.
[9] Zerbi G, Ciampelli F, Zamboni VJ. Polym Sci 1963;C7:141.
[10] Kobayashi M, Akita K, Tadokoro H. Makromol Chem 1968;118:324.
[11] Kissin YV, Rishina LA. Eur Polym J 1976;12:757.
[12] Hanna LA, Hendra PJ, Maddams W, Willis HA, Zichy V, Cudby MEA. Polymer 1988;29:1843.
[13] Kissin YV, Tsvetkova VI, Chirkov NM. Vysokomol Soedin 1968;A10:1092.
[14] Kissin YV. Adv Polym Sci 1975;15:92.
[15] Miyamoto T, Inagaki H. J Polym Sci 1969;A2(7):963.
[16] Zhu XY, Yan DY, Yao HX, Zhu PF. Macromol Rapid Commun 2000;21:354.
[17] Zhu XY, Yan DY. Macromol Chem Phys 2001;202:1109.
[18] Zhu XY, Li Y, Yan DY, Zhu P, Lu Q. Colloid Polym Sci 2001;279:292.
[19] Zhu XY, Yan DY, Fang YP. J Phys Chem B 2001;105:12461.
[20] Alamo RG, Kim MH, Galante MJ, Isasi JR, Mandelkern L. Macromolecules 1999;32:4050.
[21] Alamo RG, VanderHart DL, Nyden MR, Mandelkern L. Macromolecules 2000;33:6049.
[22] VanderHart DL, Alamo RG, Nyden MR, Kim MH, Mandelkern L. Macromolecules 2000;33:6078.
[23] Thomann R, Wang C, Kresssler J, Mulhaupt R. Macromolecules 1996;29:8425.
[24] Thomann R, Semke H, Maier RD, Thomann Y, Scherble J, Mulhaupt R, et al. Polymer 2001;42:4597.
[25] Turner-Jones A. Polymer 1971;12:487.
[26] Bruckner S, Meille SV, Petraccone V, Pirozzi B. Prog Polym Sci 1991;16:361.
[27] Weng WQ, Hu WG, Dekmezian AH, Ruff CJ. Macromolecules 2002;35:3838.
[28] Langston J, Dong JY, Chung TC. Macromolecules 2005;38:5849.
[29] Kissin YV, Tsvetkova VI, Chirkov NM. Eur Polym J 1972;8:529.
[30] Natta G, Corradini P. Nuovo Cimento Suppl 1960;15:40.
[31] Bruckner S, Meille SV. Nature 1989;340:455.
[32] Meille SV, Bruckner S, Porzio W. Macromolecules 1990;23:4114.
[33] Turner-Jones A, Aizlewood JM, Beckett DR. Makromol Chem 1964;75:134.
[34] Auriemma F, De Rosa C, Boscato T, Corradini P. Macromolecules 2001;34:4815.